Chapter 17
Green Composites for Application in Antistatic Packaging

Leonardo de Souza Vieira, Isabela Cesar Oyama, Larissa Stieven Montagna, Mirabel Cerqueira Rezende, and Fabio Roberto Passador

1 Introduction

1.1 Antistatic Packaging

The generation and accumulation of electrostatic charges are the main problems encountered in the production and operation processes in the electronics industry. Electronic components, boards, and integrated circuits are very sensitive to electrostatic voltages generated by friction with their packaging and can be completely damaged when transported, stored, or handled incorrectly [22, 57]. The generation of electrostatic charges by friction (or triboelectrification), when not properly controlled, can even lead to the risk of fires or small explosions if there are gases, vapors, or flammable powders in the factory environment [64, 69]. Estimates show that, in the USA, 5% of the market related to the sale of electronic devices is affected by losses caused by electrostatic discharge (ESD) damages [57].

In this way, the development of new materials and production processes which mitigate the problem of generation and accumulation of electrostatic charges in the electronics industry represent a reduction in operating risks and production costs. Moreover, it is obtained an improvement in product quality and reliability, guaranteeing plain customer satisfaction and resulting in fewer expenses in repairing goods, which increases the profits obtained by the company.

The packaging used to protect electronic devices against ESD is called *antistatic packaging* and is used in large volumes in the electronics industry [57]. Antistatic packaging must present a sufficiently low electrical resistivity in order to dissipate electrical charges through their structure [54]. Antistatic materials present electrical

L. de S. Vieira · I. C. Oyama · L. S. Montagna · M. C. Rezende · F. R. Passador (✉)
Polymer and Biopolymer Technology Laboratory (TecPBio), Federal University of São Paulo (UNIFESP), 330 Talim St., São José dos Campos Zip code 12231-280, Brazil
e-mail: fabio.passador@unifesp.br

S. Thomas and P. Balakrishnan (eds.), *Green Composites*,
Materials Horizons: From Nature to Nanomaterials,
https://doi.org/10.1007/978-981-15-9643-8_17

resistivity in the range 10^3–10^{10} Ω m [18]. The norms regarding the establishment of standards for the control and protection of equipment susceptible to damage by electrostatic discharge are developed and disseminated by different organizations, including the ESD Association. This organization is accredited by the American National Standards Institute (ANSI) and represents the USA in the International Electrotechnical Commission (IEC), an institution organized by the international community for the development of a series of documents regarding the establishment of standards for the ESD control. These documents receive the general designation IEC 61340 and are technically equivalent to the ANSI/ESD S20.20 standard, developed by the ESD Association [18].

Antistatic packages are generally produced with non-biodegradable polymers of fossil resource, such as polyethylene (PE) [58] and poly(ethylene terephthalate) (PET) [64]. Thus, the production of packaging obtained from renewable resources and biodegradable materials constitutes a promising research area, attracting several companies and generating large investments in the development of more sustainable alternatives [6, 49].

For example, a promising alternative to the use of conventional low-density polyethylene (LDPE) obtained from fossil resources is the use of green low-density polyethylene (green LDPE), in which the main raw material is sugar cane, that is, a material from a renewable resource. The growth process of sugar cane consumes CO_2 present in the atmosphere and, in this way, contributes to reduce the amount of this greenhouse gas in the environment. Green LDPE presents similar properties and performance presented by petrochemical-based PE, which favors industrial interests in this material [46].

Among the biodegradable polymers available to produce biodegradable packagings are polycaprolactone (PCL) [27], poly(lactic acid) PLA [65], and poly(hydroxybutyrate-*co*-hydroxyvalerate) (PHBV) [12]. Besides green LDPE, PHBV is also a material obtained from renewable resources that is widely studied due to its good biodegradability and biocompatibility. Furthermore, PHBV has physical and mechanical properties similar to PE and polypropylene (PP) [2, 32, 35, 71].

Antistatic packages produced from insulating polymeric matrices, such as green LDPE and PHBV, need modification in their formulation in order to decrease the electrical resistivity of the material. So, it can dissipate the electrical charges formed by the friction between the electronic device and the packaging during transport and storage of that electronic device. There are many ways to achieve this goal, and the most common technique is the addition of electrically conductive particles that leads to the formation of electron-conducting paths in the polymeric matrix [58, 64]. These electrically conductive particles may be generically called *antistatic agents* [57]. The increase in electrical conductivity with the addition of increasing levels of the conductive material has the characteristic of being nonlinear. There is a certain amount of antistatic agent that, when added to the polymeric matrix, ensures that its particles establish physical contact with each other and form a network of continuous electron conduction throughout the composite structure, with an increase of several decades of magnitude in its electrical conductivity [62]. This critical amount is called the *electrical percolation threshold* [53]. A low electrical percolation threshold is

desirable, avoiding major changes in the mechanical and rheological properties of the polymeric matrix [58, 62].

Carbon black (CB) is one of the materials most employed as antistatic agent mainly due to its relatively low cost [62, 68, 73]. Silva et al. [58] developed PLA/CB composites reinforced with different contents of CB (5, 10 and 15 wt%) using a thermokinetic mixer. Mechanical tests showed that the Izod impact strength of the composites presented a slight decrease when compared to neat PLA. Thermogravimetric analysis (TGA) showed that the addition of 10 wt% of CB increased the degradation temperature (T_{onset}) by up to 32 °C when compared to neat PLA, which was attributed to the formation of char that thermally insulated polymer chains not yet thermally degraded. The electrical conductivity test by impedance spectroscopy showed that the addition of 10 wt% of CB increased the electrical conductivity in 9 decades of magnitude which qualifies the material as a promising alternative for the production of ESD protective packaging.

Nonetheless, CB has the drawback of presenting a high electrical percolation threshold in many polymer matrices. Due to its low electrical conductivity and its low tendency to disperse, it is necessary to add a relatively high amount of this carbon material in the polymer matrix to establish an effective electron-conducting path in the polymer matrix [64, 68, 73]. Wang et al. [68] explained that, in order to obtain satisfactory antistatic properties in poly(vinyl chloride) (PVC)/CB composites, it is necessary to add up to 25 wt% of CB to the PVC matrix, which may negatively interfere with the mechanical properties of the material and impair its rheological and processing characteristics.

Another disadvantage of the use of CB is the unhealthy aspect related to its production and handling, which involves the generation of many nanoparticles suspended in the air and respiratory problems in those who inhale them [44].

In this way, there are various alternatives of reducing electrical resistivity of insulating polymeric materials available in the literature, which includes the use of surfactant molecules [16], metallic particles [76], oxide whiskers [75], polymer electrolytes [14], the addition of intrinsically conducting polymers such as polypyrrole and poly (3, 4-ethylenedioxythiophene) [33], use of conductive ionomers [39], and the addition of carbon materials such as carbon nanotubes [9, 19], graphene [74], and graphite nanoparticles [47].

1.2 Methods to Obtain Polymeric Materials with Antistatic Properties

An interesting way of increasing the electrical conductivity of electrically insulating polymers constitutes the addition of organic antistatic agents such as ionic and non-ionic surfactants [5]. The molecules of surfactants with low molar weight migrate to the outermost layers of the polymer and absorb water molecules present in the atmosphere due to the hydrophilicity of its chemical groups, conferring conductive

properties to the surface of the material [67]. An example of an antistatic agent used in the production of materials with dissipative properties is ionic liquids, which basically consist of molten salts at room temperature. Ionic liquids have interesting properties because they are not volatile and flammable and present high thermal stability and high ionic density [16]. Ding et al. [16] developed a material with promising antistatic characteristics from the addition of 1-n-tetradecyl-3-methylimidazolium bromide ([C14mim] Br) in PP polymer matrix with a weight ratio of 100/3. A good dispersion of [C14mim] Br in the polymer matrix was reported, indicating good chemical compatibility between the two phases. The addition of [C14mim] Br molecules increased the impact resistance of PP, which was attributed to its effect of a nucleating agent in the polymeric matrix, refining the structure of its spherulites. Electrical conductivity tests showed that the addition of the antistatic agent led a decrease of 7 decades of magnitude in the electrical resistance of PP (from 2.67×10^{14} Ω to 2.60×10^{7} Ω), obtaining a material with promising antistatic properties. However, this technique presents a reduction in the dissipative properties over time as the molecules of the antistatic agent migrate and deteriorate on the surface [67]. Another negative issue is the effectiveness dependence of the packaging in relation to the relative humidity of the air [69].

Zhou et al. [75] prepared PVC/zinc oxide whiskers (ZnOw) composites with different ZnOw contents (1, 2, 3, 4, 5, and 6 wt%) to obtain materials with antistatic properties. Zinc oxide whiskers (ZnOw) are ceramic materials with a semiconductive character and are shaped like fine needles that grow in four different directions and form a three-dimensional structure. Within the polymer, adjacent needles that overlap are able to guarantee a flow of electrical charges through the composite and increase the electrical conductivity of the polymer matrix. Results of electrical tests indicated that the addition of 6 wt% of ZnOw can lead to a reduction in the electrical resistivity of 6 decades of magnitude and can be a promising material for ESD protection. The addition of ZnOw in another polymeric matrix (PP, in this case) allows obtaining composites with equally attractive properties. The addition of 3 wt% of ZnOw decreases the electrical resistivity of neat PP from 10^{16} Ω cm to 10^{9} Ω cm, which represents a considerable reduction of 7 decades of magnitude in this electrical property [60].

The formation of gel polymeric electrolytes constitutes another alternative of obtaining materials with electrically dissipative characteristics. Gel polymer electrolytes are dimensionally stable and are developed basically by the introduction of an ion-conducting mechanism inside electrically insulating polymers [14]. Che et al. [14] prepared composites with PVC as polymer matrix and the addition of bis [2-(2-methoxyethoxy ethyl] phthalate (BMEP doped with sodium thiocyanate salt (NaSCN. Composites were processed using a torque rheometer, and different contents of BMEP/NaSCN (or AP) were investigated. The Na^{+} cation dissociates from the salt and establishes a coordination effect with the oxygen atoms of the ether groups present in the BMEP structure. With the appearance of a potential difference, mobile cations migrate through percolative paths established by the network of BMEP molecules mixed inside the PVC matrix, which can collaborate to increase the electrical conductivity of the material. Electrical conductivity tests showed a low

electrical percolation threshold (~20 AP phr), and a decrease of 7 decades of magnitude in the electrical resistivity of composites was obtained (10^{15} Ω sq^{-1} (0 phr AP) to 10^{8} Ω sq^{-1} (60 phr AP)). The effect of the addition of 40 phr of dibutyl phthalate (DBP) plasticizer to the PVC/AP composite was also verified. The addition of DBP promoted a further reduction in the electrical resistivity of PVC/AP composite. This phenomenon was attributed to the plasticizing effect that DBP imparts to the PVC polymeric chains, reducing its rigidity and facilitating the transfer of charge carriers (Na^{+}). Electrical tests were also carried out by varying the relative humidity (RA) from 50 to 0%, and it was verified that the electrical resistivity of the composites reduced only one decade of magnitude, indicating that an advantage of this method consists in obtaining materials that do not depend on this environmental condition to acquire dissipative properties.

Among the methods previously mentioned to produce antistatic packages, Maki et al. [39] evaluated the production of antistatic packages using a different way, which is without mixing or coating the polymer with an antistatic agent. Low resistivity was reached using an ionomer of a copolymer of ethylene with potassium as the metal ion type with other host resins. Generally, the ionomer has sodium or zinc ions in its chain that do not promote antistatic properties. The change with the addition of potassium helps to increase electrical conductivity. The authors developed a random ethylene copolymer (derived from polymerization of ethylene-comethacrylic and acid isobutyl acrylate) in which carboxylic groups (about 80%) were neutralized with potassium resulting in the production of the ionomer. A multi-layer cast film machine was used to produce films with single and multi-layer of potassium ionomer, metallocene linear low-density polyethylene (mLLDPE) with an antistatic agent and potassium ionomer/mLLDPE so as to characterize antistatic properties. The static decay time, surface resistivity and volumetric resistivity and space charge distribution (pulsed electroacoustic method) tests were evaluated. Static decay time test proved that potassium ionomer has rather good static decay properties compared to mLLDPE with an antistatic agent. It means that antistatic properties can be found on the surface of the film if potassium ionomer is added in any desired layer. The same behavior occurs with mLLDPE containing the antistatic agent. The stable performance of the ionomer was gain in the multi-layer structure instead of the single layer. The study of a two-layered film (one layer is the potassium ionomer, and the other is mLLDPE) was essential to understand the reason why multi-layered structures present good antistatic properties. The authors concluded that the use of potassium ionomer in antistatic packaging is satisfactory because it showed antistatic properties equal to polymeric composites with antistatic agents.

Jonas and Heywang [33] developed a method to coat plastic films with polypyrrole. Polypyrrole is an infusible and insoluble conductive polymer due to branching in its chain, so it was of great meaning finding a methodology to produce antistatic packaging from plastic film coated with polypyrrole. Antistatic packaging must have low electrical surface resistivity, and its antistatic characteristic cannot change by atmospheric humidity and need to be stable for at least four weeks at 70 °C. Besides that, the authors produced films of polypyrrole-coated polycarbonate following three steps. The materials used were a film of polycarbonate, polyvinyl

acetate with ferric salt, and pyrrole monomer. The production of polypyrrole-coated polycarbonate follows the following procedure. The pyrrole monomer was polymerized at the polyvinyl acetate surface, and a conductive polymer was created and coated the polycarbonate film; it is important to frame that the polymer resulted from coating process is thermoformable. The coating procedure enabled an electrical surface resistivity of 10^3–10^4 Ω m^{-1}; thus, this low surface resistivity allows the use of the film in antistatic packaging.

In general, the mechanism of surfactant antistatic agents in packages is based on the migration of them to the film surface when humidity is absorbed on the polymeric surface. Therefore, humidity is essential to trigger the antistatic role, even at low percentages. Besides electrical properties, antistatic packaging demands flexibility in order to facilitate processing and minimizing defects of the final product. Up to recent years, plasticizer derived from phthalate had been used mainly, but it has the problem associated with its toxicity, which can lead to utterly hazardous diseases.

Linking the necessity of a non-harmful plasticizer and antistatic charge, Wang et al. [70] engineered an eco-friendly biodegradable antistatic agent and plasticizer to produce antistatic composites with the polymeric matrix. PVC/citrate electrolyte-based antistatic plasticizer (CEAP)/tributyl citrate (TBC) composite was produced. TBC is a biodegradable and non-toxic plasticizer. Foremost, the synthesis of CEAP was made reacting citric acid, 2-butoxyethano, and sodium thiocyanate through an esterification reaction. The composites were prepared in a torque rheometer with a temperature of 160 °C, rotor speed of 30 rpm, and blending time set of 6 min. In general, a decrease of two decades of magnitude in superficial resistivity at room temperature was observed. Besides that, a reduction of one decade of magnitude in electrical superficial resistivity was reached increasing the temperature (40–80 °C). No significant modification at surface resistivity occurred changing relative humidity. The composite without TBC showed insufficient antistatic properties; thus, TBC is essential as a plasticizer and contributes to ion's mobility in polymer chain decreasing electrical surface resistivity.

Another way to produce antistatic packaging is the addition of metal fillers in the polymeric matrix due to their permanent electrical conductivity and low cost [76].

The addition of carbon materials to insulating polymers is the most used technique for obtaining antistatic packaging. Carbon materials are suitable for the most varied applications since carbon atoms are capable of forming materials with distinct crystalline structures and versatile and attractive properties [62]. Among the carbon materials studied and employed in dissipative materials to replace carbon black are the carbon nanotubes [9, 19], graphene [74], graphite [47], and, more recently, glassy carbon [46, 54, 63].

Carbon nanotubes and graphene are relatively recent and promising alternatives to replace carbon black since they confer excellent mechanical, thermal, and electrical properties to polymers [68]. Huang et al. [26] developed cellulose nanocomposites reinforced with different contents of carbon nanotubes (CNT) (1, 3, 5, 8 and 10 wt%) using a sequential solution dispersion, gelation, and hot-press drying process. The use of cellulose in the production of composites for applications in antistatic packaging is very promising, aiming at the substitution of polymers from non-renewable

resources. The electrical percolation threshold occurs with the addition of 0.71 wt%, and the addition of 5 wt% of CNT to the cellulose increased the electrical conductivity from 10^{-13} S m^{-1} to only 5.6 S m^{-1}, obtaining an electrically dissipative material. Therefore, it is possible to obtain antistatic properties with a much lower amount of filler compared to carbon black.

Notwithstanding its good properties, carbon nanotubes and graphene present a high specific surface area (due to its nanoscale dimension) and a strong van der Waals interaction established between its nanofillers, which increases the tendency of agglomeration and hinders the distribution and dispersion processes of these materials in the polymer matrix, impairing the properties of composites [24]. Another disadvantage presented by carbon nanotubes is their high stable surface and their hard surface, which impairs the interaction between the polymer matrix and the nanofiller and the transfer of mechanical stress among these phases. For this reason, it is common the use of chemical/physical treatments in CNT to modify its surface properties by the introduction of polar functional groups to the nanofiller. The increase in the polarity of CNT may facilitate its interaction with polymeric chains in polymeric composites, increasing the mechanical properties of the material [36]. However, it may lead to a loss in the electrical and mechanical properties of CNT.

In this way, the need to search for an alternative material to the carbon black fosters the interest of novel materials that can be employed in the production of polymeric materials with antistatic properties. Although there are few studies in the literature on the use of glassy carbon (GC) as a filler in polymeric matrices, it is verified that this material gives good mechanical and electrical properties to polymers, making it a promising material in the production of antistatic packaging [46, 54].

Szeluga et al. [63] prepared composites with 5, 10, and 20 wt% of GC in epoxy resin (EP) and hybrid composites with the addition of GC and multiwall carbon nanotubes (MWCNT). It was verified that GC presents a good adhesion to the polymeric matrix, which explains its good dispersion and distribution. It was verified that the binary composites of EP/GC with 10 wt% GC presented an electrical resistivity of 3.02×10^{7} Ω cm, 7 decades of magnitude lower than the neat EP (4.82×10^{14} Ω cm). The addition of 0.25 wt% MWCNT led to a further decrease in the electrical resistivity of the material (1.68×10^{3} Ω cm), indicating a synergistic effect between the carbon fillers.

The use of GC in thermoplastic polymer matrix composites for the production of antistatic packaging has also shown to be a very promising alternative. Santos et al. [54] produced composites of low-density polyethylene (LDPE) with different contents of GC (0.5, 1, 5, 10, 15, and 20 wt%) using a thermokinectic mixer. It was observed that GC particles are well-dispersed and distributed in the polymer matrix, making it possible to obtain a relatively low electrical percolation threshold with the addition of 0.5 wt% GC. A decrease of 2 decades of magnitude in the electrical resistivity was also observed. The composite with 0.5 wt% GC presented the best optimization of mechanical and thermal properties, comparable to neat LDPE, which demonstrates that GC is a promising alternative of an antistatic agent in replacement to CB.

Oyama et al. [46] verified that low electrical resistivity was reached using contents of GC below 0.5 wt% in a green polymeric matrix, green LDPE. GC contents of 0.1, 0.3, and 0.5 wt% were used in the green LDPE matrix. The materials were mixed in a thermokinetic homogenizer. A reduction of 6 decades of magnitude in electrical resistivity (from 10^{14} to 10^{8} Ω m) was reached with the addition of only 0.1 wt% of GC in green LDPE/GC composite. A reduction of 7 decades of magnitude in the electrical resistivity was verified with the addition of 0.3 and 0.5 wt% GC. It indicates that small contents of GC are able to produce conductive paths in the green polymeric matrix.

As it is perceived in the examples previously mentioned, there are many works present in the literature involving the obtainment of materials with antistatic characteristics produced with polymers originated from non-renewable resources, such as PVC, PE, and PP. However, it is also noticed the use of polymers obtained by renewable resources and/or biodegradable polymers.

In this chapter, we will show the effectiveness of using green composites for the production of antistatic packaging. The antistatic agent chosen is the glassy carbon because it is from a renewable resource. The polymeric matrices used for the production of the green composites were a biodegradable polymer and a polymer from a renewable resource.

1.3 Glassy Carbon: A Green Antistatic Agent

Glassy carbon (GC), also named as vitreous carbon, is a carbon and isotropic material that generally presents both high hardness and elastic modulus, elevated chemical inertness, and temperature resistance. It is commonly obtained from the carbonization of certain thermoset resins, such as phenolic and polyfurfuryl alcohol (PFA) resins, at temperatures normally above 1000 °C in inert atmosphere [11]. Polyfurfuryl alcohol resin, also named as furfuryl resin, is originated through the polymerization of furfuryl alcohol, which can be obtained from the catalytic hydrogenation process of furfural. Furfural consists of a heterocyclic and aromatic aldehyde produced by dehydrating pentoses present in lignocellulosic biomass of plants and residual materials, such as corncobs, rice husks, and sugar cane bagasse [41]. In this way, GC produced from furfuryl resin constitutes a green material, since it is originated from renewable resources. When treated at high temperatures, the precursor resins of GC lose considerably the content of oxygen, hydrogen, and nitrogen present in their polymer chains, leaving high carbon content in their chemical composition (at least 90% by mass). The resulting carbon material has the term vitreous in its designation for having a shiny appearance when polished and for having a fracture surface similar to that presented by the glass [21].

GC belongs to the carbon materials class that is arranged by stacking of hexagonal planes of C with sp^2 hybridization, which is called graphitic materials [28]. Graphite presents the most well-organized basic structure among graphitic materials. The distance between its graphitic planes is 0.3354 nm, and the distance between the C

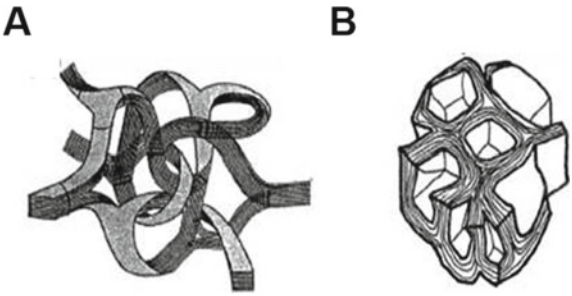

Fig. 1 Schematic representation of the GC structure according to **a** the Ribbon Model and **b** the Shell Model [28]

atoms in the plane is 0.1412 nm [28]. Carbon materials obtained under heat treatment at temperatures below 1300 °C have reduced levels of regularity in the stacking of the graphitic planes. Thus, the length of these plans tends to be small, as well as the number of hexagonal plans stacked. The arrangement of atoms formed in these materials, with lower order than that present in graphite, is called *turbostratic structure* [28]. The submission of graphitizable carbon materials to heat treatments at temperatures above 1700 °C can lead to an improvement in the organization of the turbostratic structure and an increase in the size and number of stacked planes. This process is called *graphitization*. However, in carbon materials classified as *non-graphitizable* (e.g., GC), the stacking of the graphite planes is highly disorganized and linked by disorganized carbons, and thus, it is not possible to obtain a graphite structure even when subjected to heat treatments at high temperatures [28].

Among the structural models proposed for the GC are the *Ribbon Model*, proposed by Jenkins and Kawamura (Fig. 1a), and the Shell Model, proposed by Shiraishi (Fig. 1b) [28, 30]. The Ribbon Model proposes that this carbon material consists of a network of folded and twisted carbon layers [30]. This model, however, is ineffective in explaining some GC properties, such as its high porosity (closed pores) and its low gas permeability. The Shell Model, however, elucidates this issue by presenting the microstructure of the GC as layers of hexagonal carbon arrangements that form closed structures (pores) [28].

GC has good chemical and mechanical resistance, high hardness, high modulus of elasticity (20–40 GPa), high electrical (~10^4 S m^{-1}) and thermal conductivities, and good gas impermeability [29, 45, 56]. These characteristics make this material suitable for a wide variety of applications, including heart valves, electrodes, refractory applications, catalyst supports, and others [8, 29, 34].

GC can be obtained, basically, in the form of reticulated glassy carbon (RGC) or monolithic glassy carbon (MGC) (Fig. 2a, b, respectively). RGC consists of a macroporous material with many accessible pores (as shown in the zoom of Fig. 2a) and a high surface area in relation to its volume, presenting high chemical stability, lightweight, and low cost [45]. The most common applications for RGC include water purifiers, gas separators, electrodes, natural gas stores, and biological growth supports [25, 51].

Another common form of GC is MGC, whose structure is characterized by the presence of a predominant amount of micro- and mesopores [21]. The diffusion

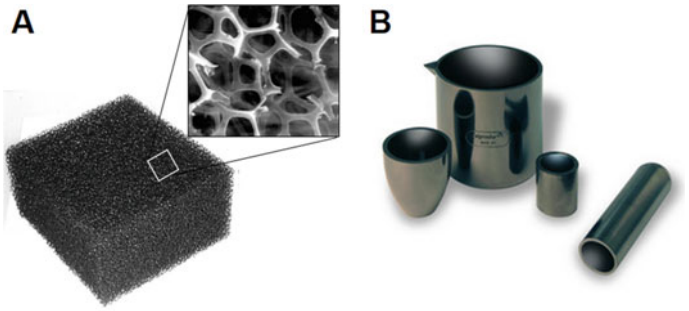

Fig. 2 Reticulated glassy carbon (RGC) (**a**) and monolithic glassy carbon (MGC) (**b**) [20], SPI [61]

of volatiles and the shrinkage of the material under heat treatment can lead to the formation of tensions and discontinuities in its structure. In this way, the heating rate must be strictly controlled, limiting the thickness of the piece obtained [8]. Its high purity and its physicochemical properties make MGC an interesting choice for the production of special crucibles (Fig. 2b) and tubes, catalyst supports, gaskets, electrodes, heart valves, among others [31].

1.4 Green Polymer for the Production of Antistatic Packaging

The production of polymeric materials from renewable resources gained great notoriety in the 1970s during the oil crisis. At this time, the price of oil barrels had a great increase, as well as the price of the products obtained from petroleum [36]. Since then, the production of polymers from renewable resources has received massive investments in science and in the industrial sector [6, 49].

Technological development in the area of biodegradable polymers has also obtained remarkable prominence in recent years due to the potential risk that the disposal of plastics can cause to the environment and to the most diverse ecosystems around the world. The application of plastic is widespread in practically all areas of the productive sector, and it is especially important in the packaging industry since it consumes around 44.8% of all plastic produced annually [23]. The antistatic packaging generally constitutes a single-use product. PP and PE are the most used polymers in the production of packaging and present high chemical stability and durability. This high chemical stability is a common characteristic of conventional polymers of fossil resource, making the biodegradation rate of these materials relatively low. It is estimated that, since 1950, about 79% of the plastic produced in the world is still present in landfills or in the environment [52].

Table 1 General properties presented by Green LDPE (SBF0323HC grade) [10]

General properties	Value	Unit
Melt flow rate (190 °C/2.16 kg)	0.32	g/10 min
Density	0.923	g/cm^3
Tensile strength at break	20	MPa
Elongation at break	390	%

1.4.1 Green Low-Density Polyethylene (Green LDPE)

Polyethylene is one of the most used polymers in the world due to its excellent mechanical properties and low density. The main applications include the production of many types of packaging, car fuel tanks, wire, and pipes.

A Brazilian petrochemical company developed a different route to produce PE changing the oil-base origin to a green one [43]. Green LDPE is produced by renewable feedstock, sugar cane, and has the same properties, processing and recyclability possibilities as petrochemical LDPE. The green LDPE presents low electrical conductivity, excellent thermal, mechanical properties, and great water vapor impermeability. Table 1 shows green LDPE properties. Summarizing, the process consists in producing ethylene monomer from ethanol extracted from sugar cane. This is an eco-friendly environmental process due to the capture of an enormous quantity of CO_2 from the atmosphere by sugar cane [43]. Besides this, sugar cane has been also using to produce fuels for automobiles [15]. In this way, this material participates in a green cycle.

Ethanol can be obtained from a variety of sugary feedstock like sugar cane, cornstarch, cassava, potato, and sugar beet. Brazil is one of the leaders of sugar cane production. This fact facilitates the continuous production of green polymers due to the abundance of feedstock material, which reduces the cost linked to production, and ease of logistics. Ethanol's obtaining route consists of fermentation of sugar cane stalk, followed by a catalytic dehydration reaction to produce ethylene, which has exactly the same chemical structure as ethylene from fossil origin. Then ethylene is polymerized to obtain green LDPE. It is worth mentioning that the same polymerization reactor used for petrochemical LDPE can be used to polymerize green LDPE [43].

1.4.2 Biodegradable Polymer for the Production of Antistatic Packaging

Many biodegradables polymers have been proposed to replace petroleum-based polymers in industry, such as cellulose [26], PCL [27], PLA [65], and polyhydroxyalkonates (PHAs) [12, 35, 66].

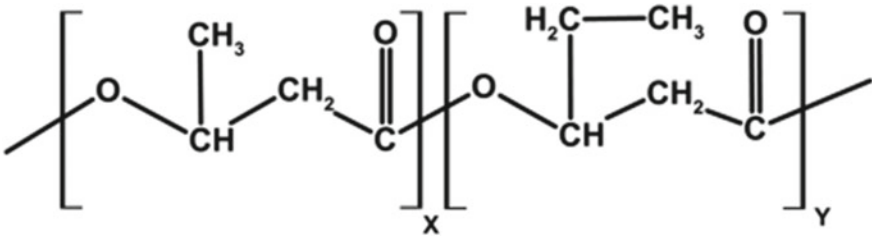

Fig. 3 Schematic representation of the PHBV chemical structure. *Source* Author

Table 2 General properties presented by PHBV (PHI 002)

General properties	Value	Unit
Melt flow rate (190 °C/2.16 kg)	5 to 10	g/10 min
Density	1.23	g/cm^3
Tensile strength at yield	18.7	MPa
Tensile elongation at yield	1	%
Tensile maximal strength	39.6	MPa
Tensile strength at break	39.6	MPa
Elongation at break	3.2	%

PHAs are basically polyesters of high molar weight that possess good biodegradability and biocompatibility [1]. Among PHAs is the poly(hydroxybutyrate-*co*-hydroxyvalerate) (PHBV), a polymer that presents properties similar to those observed for conventional polymers, such as PE e PP [2, 32, 35, 71].

Poly (Hydroxybutyrate-co-Hydroxyvalerate) (PHBV)

PHBV constitutes a statistical copolymer of mere hydroxybutyrate (HB) with random segments of mere hydroxyvalerate (HV) (Fig. 3) [35]. PHBV is produced during the bacterial fermentation of sugars for the production and accumulation of energy reserves in intracellular granules [50]. In industry, PHBV can be synthesized in large bioreactors through bacterial fermentation of propionic acid and glucose. The originated polymer can be captured and purified through the use of a specific solvent, obtaining a solid and dry final product [48, 50]. The general properties presented by PHBV are shown in Table 2.

PHBV presents a high rate of biodegradation since its ester bonds are easily hydrolyzed by the action of bacteria and fungi, generating compounds of smaller molar mass [13]. Biodegradation is an irreversible process of deterioration of a material, causing structural modification and alteration in the chemical and mechanical properties [38]. This process occurs through the enzymatic action of microorganisms (such as bacteria and fungi) that use the product of degradation as resources of energy, electrons, and atoms (e.g., carbon, nitrogen, oxygen, phosphorus, sulfur, etc.),

which are necessary for the maintenance of their cellular activities [37]. Among the bacteria involved in the biodegradation process of PHAs, it is possible to mention the species *Alcaligenes faecalis T1*, *Pseudomonas lemoignei*, *Pseudomonas fluorescens GK13*, *Streptomyces exfoliates K10*, *Comamonas testosterone*, *Comamonas acidovorants*, etc. As an example of fungi capable of biodegrading PHAs are *Aspergillus penicilloides*, *Aspergillus fumigatos*, *Penicillium funiculosum*, *Penicillium daleae*, *Paecilomyces marquandii*, *Candida guilliermondii*, etc. [36].

The biodegradation process can occur inside the cells of the microorganisms that naturally produce PHAs or outside the cells of microorganisms that do not produce PHAs [36]. The high molar weight of the polymeric chains and their low hydrophilicity make it difficult for whole macromolecules to enter the cells of these microorganisms; therefore, it is necessary that the degradation occurs initially in an external environment. The process begins with the formation of a layer of water and excreted enzymes (*depolymerases*) called biofilm, where the polymeric chain is broken down [36]. In PHBV biodegradation, the ester bonds of the polymer chains are repeatedly hydrolyzed forming monomers HV and HB, which are soluble in water and have a molar weight small enough to enter the cell wall through passive diffusion. In general, monomers are metabolized inside cells during the tricarboxylic acid cycle and through β-oxidation, generating energy for cellular functioning [55].

In the presence of O_2, the complete process of biodegradation (mineralization) leads to the metabolization of polymer macromolecules into carbon dioxide (CO_2), water, and new cell biomass. In the absence of O_2 (anaerobic biodegradation), the production of CO_2 is replaced by the generation of methane (CH_4) [49].

2 Experimental Section: Production of Green Composites for Antistatic Packaging and Properties Analysis

2.1 Obtainment Process of Glassy Carbon, Milling and Structural Characterization

GC was obtained by the cure of PFA resin using as catalyst a 3% wt/wt aqueous solution of p-toluenesulfonic acid (APTS) (60% wt/vol.). The PFA cure was realized in four steps: at 60 °C for 24 h, at 80 °C for 2 h, at 110 °C for 2 h, and at 180 °C for 6 h. The cured PFA resin was subsequently subjected to a thermal carbonization treatment from room temperature up to 1000 °C at 10 °C min^{-1} under an inert N_2 atmosphere (1.0 L h^{-1}). The sample was kept at final temperature for 30 min and then cooled to room temperature.

GC plates (Fig. 4a) were ground in an IKA mini mill (model A11), for approximately 10 min to produce GC particulate (Fig. 4b). GC with particle size of around 75 μm was obtained using 200 mesh metal sieves.

Particulate GC was structurally analyzed on a Rigaku Ultima IV X-ray diffractometer (PANalytical, X'pert Powder model), operating at 40 kV and 30 mA with

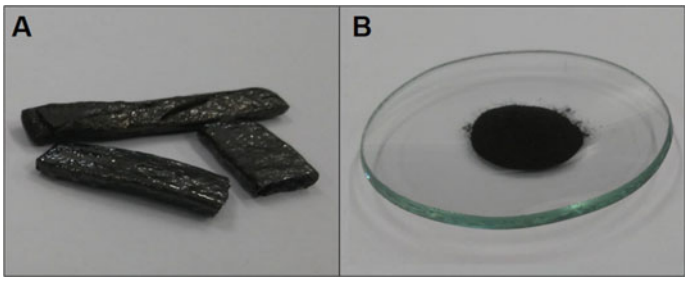

Fig. 4 Glassy carbon, in plate form (**a**), and the particulate material obtained after the milling process (**b**). *Source* Author

CuKα radiation ($\lambda = 1.54056$ Å) at a scan rate of 5° min^{-1} varying 2θ from 5° to 70°.

2.2 Processing of Green LDPE/GC Composites

Neat green LDPE (SBF0323HC grade, Braskem, Brazil) and LDPE/GC composites with 0.1, 0.3, and 0.5 wt% of GC were prepared in a thermokinetic homogenizer (MH50-H, MH Equipamentos Ltda—Brazil) with rotation of 3000 rpm and 185 °C during 30 s. After this processing, thin films (with 150 μm thickness) were produced by hydropneumatic press (PR8HP, MH Equipamentos—Brazil) at 180 °C with a pressure of 2 bar for 3 min. Thin films (0.6 mm) were used for electrical and thermal tests. Also, standardized specimens (3.2 mm) to tensile test were produced at the same equipment and temperature, with a pressure of 5 bar for 5 min.

2.3 Processing of PHBV/GC Composites

Neat PHBV (PHI 002, Nature Plast, France) and PHBV/GC composites with 1.0, 2.5, and 5,0 wt% of GC were prepared in a co-rotational extruder (AX Plastics, model AX16:40DR—Brazil), with $L/D = 40$ and $D = 16$ mm (screw thread). The thread rotation was 100 rpm, and the feeder rotation was 30 rpm. The temperature profile set in the extruder for each heating zone was 165 °C, 170 °C, 170 °C, 170 °C, and 165 °C. The material obtained was subsequently pelletized. After this processing, thin films (with 150 μm thickness) were produced by hydropneumatic press (PR8HP, MH Equipamentos—Brazil) at 190 °C with a pressure of 1 bar for 3 min.

2.4 Mechanical, Thermal, Electrical, and Biodegradability Tests

The mechanical behavior of the composites was evaluated by tensile tests according to ASTM D638-14 [3] for green LDPE composites and ASTM D 882-18 [4] for PHBV composites.

Specimens were performed in an MTS Criterion testing machine (model 45, Brazil), with a load cell of 50 kN and strain rate of 40 mm/min. The films were performed in an MTS Criterion testing machine (model 42, Brazil), with a load cell of 250 N and an initial strain rate of 0.1 mm/mm/min. At least seven samples of each composition were tested.

The thermal behavior composites were evaluated by differential scanning calorimetry (DSC) in a DSC Q2000 (TA Instruments, Brazil) equipment using small amounts (<10 mg) of dried samples that were placed into aluminum pans. The heating cycle was performed from room temperature to 200 °C with a heating rate of 10 °C min^{-1} under N_2 atmosphere. The degree of crystallinity (X_c) was calculated according to Eq. 1:

$$X_c(\%) = \frac{\Delta H_m}{\Delta H_m^\circ} \times \frac{1}{(1-\varphi)} \times 100 \tag{1}$$

where X_c is the degree of crystallinity, ΔH_m is the fusion enthalpy obtained by DSC, ΔH_m° is the fusion enthalpy of the 100% crystalline polymer (for PHBV ΔH_m° = 146 J g^{-1} [40] and for green LDPE ΔH_m° = 293 J g^{-1} [72]) and φ is the content of GC added to the composite.

The electrical characterization was performed on a Solartron Impedance/gain–phase impedance analyzer (model SI 1260, Brazil) to measure alternating current electrical resistivity by impedance spectroscopy. It produced a metal-nanocomposite-metal structure by depositing a thin layer of gold/palladium alloy on both sides of the samples using a metallizer (MED020 Bal-tec, Brazil) in order to form the electrical contact. The electrical resistivity of the materials was calculated using the thickness (l), contact area (A) values of the samples, and the impedance value (Z) obtained by the analysis, as indicated by Eq. 2:

$$\rho = \frac{Z \times A}{l} \tag{2}$$

The biodegradation test in aqueous medium was performed only for neat PHBV and PHBV/GC composites based on the methodology developed by Silva et al. [59]. The microorganisms involved in the biodegradation test were extracted from vegetal soil. In summary, samples of neat PHBV and PHBV/GC composites were immersed in 20 mL of a mineral solution containing mineral salts necessary to microorganisms cell development. Subsequently, an amount of a microbial solution (containing the microorganisms extracted from the soil) necessary to obtain a final solution with

microorganism concentration (cell mass/L) of 0.025 g L^{-1} was added to the mineral solution. The test was carried out in Falcon tubes (50 mL) under stirring (120 rpm) at 30 °C in a shaker New Brunswick™ (model Innova® 44/44R) with semi-open Falcon tubes for gas exchange. Samples were taken every 15 days during a total period of 45 test days of biodegradation in aqueous solution. It used four samples for each composition. After removal, the samples were washed with distilled water to remove material adhered to the surface and were vacuum dried.

3 Results and Discussion

Figure 5 shows the X-ray pattern obtained for GC. It is possible to observe the presence of two diffraction peaks characteristic of a turbostratic structure. The first peak is located at $2\theta = 23.6°$ and is attributed to the plane (002), which is related to the distance between the graphitic planes. The second peak is located at $2\theta = 43.4°$, attributed to the plane (10), which is associated with the in-plane structure [34, 45].

Figure 6a, b show the graphs of elastic modulus and degree of crystallinity as a function of the GC content for neat LDPE and green LDPE/GC composites and neat PHBV and PHBV/GC composites, respectively.

It is possible to verify, in relation to green LDPE/GC composites, that the increase in the GC content leads to an increase in the elastic modulus and a slight decrease in the degree of crystallinity of the green LDPE. Probably, the adhesion between the LDPE and the GC was strong enough to allow the transfer of mechanical stress from the matrix to the reinforcing phase, increasing the stiffness of the material.

There is also a decrease in the degree of crystallinity of green LDPE (up to 2.6%) with the increase in the GC content. Probably, the GC particles hindered the ordering

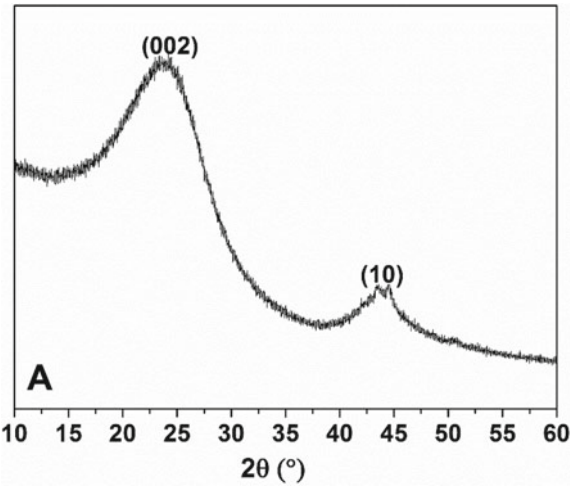

Fig. 5 X-ray pattern of GC. *Source* Author

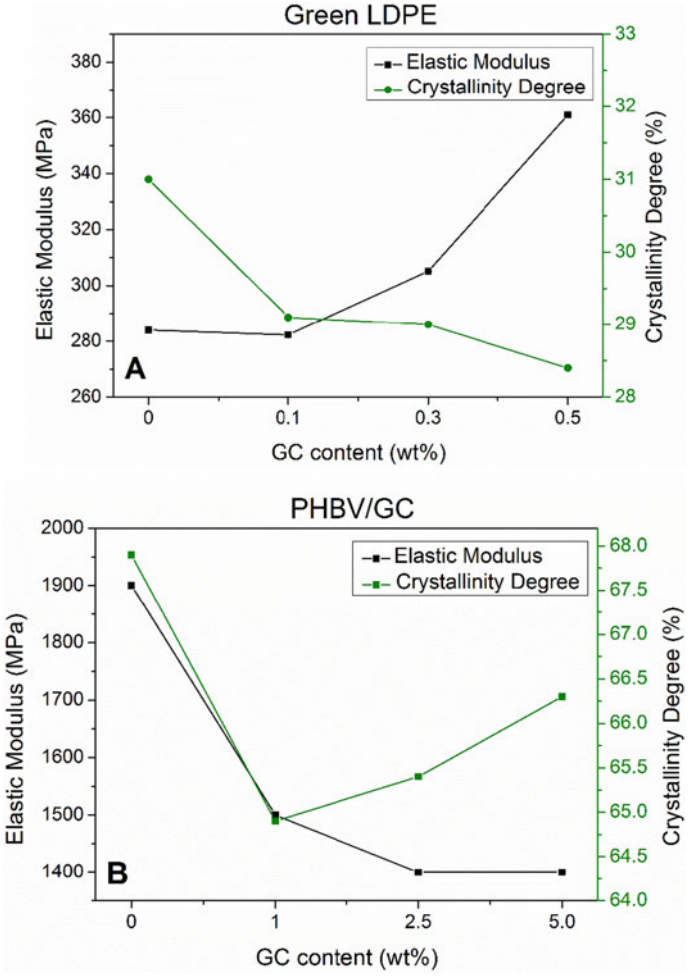

Fig. 6 Graphs of elastic modulus and crystallinity degree as a function of GC content for **a** LDPE/GC and **b** PHBV/GC composites. *Source* Author

of polymeric LDPE chains in crystallites during the crystallization process, restricting relaxation. It is suggested that a similar phenomenon occurred in PHBV present in PHBV/GC composites since in these composites the degree of crystallinity decreased up to 3% (Fig. 6b). The reduction in the crystallinity degree is the possible cause for the decrease in the elastic modulus in the material, which dropped from 1900 to 1400 MPa (PHBV/2.5 GC). The decrease in the stiffness of PHBV constitutes a positive factor for its use in the production of antistatic packaging since it is necessary a certain flexibility in the material to facilitate the handling of the package. Thus, regarding the flexibility requirements, green LDPE/GC composites have a certain

advantage over PHBV/GC composites, since they have stiffness about four times lower.

Figure 7a, b show the graphs of electrical resistivity for neat green LDPE and green LDPE/GC and for neat PHBV and PHBV/GC composites as a function of the GC content present in the composites.

The addition of 0.1 wt% GC decreased the electrical resistivity of green LDPE by 6 decades of magnitude, ranging from 1.4×10^{14} Ω m to 1.7×10^{8} Ω m. Green LDPE/GC composites with 0.3 and 0.5 wt% GC showed an electrical resistivity of 4.8×10^{7} Ω m and 2.1×10^{7} Ω m, respectively, that is, 7 decades of magnitude lower than neat green LDPE. In these composites, the GC content was sufficient for the particles of the antistatic agent to come into contact with each other, forming an

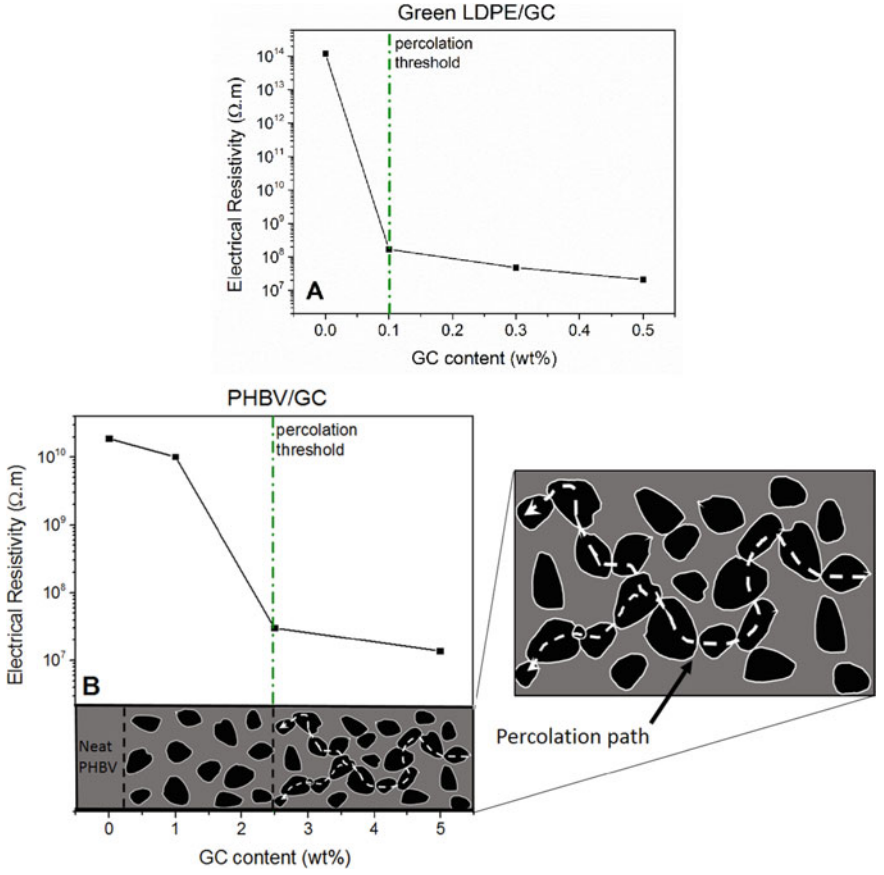

Fig. 7 Graphs of electrical resistivity as a function of GC content for **a** green LDPE/GC and **b** PHBV/GC composites with the scheme of formation of the electric percolation path. *Source* Author

electron percolation path in the material, resulting in a drastic reduction in electrical resistivity.

It can be seen in Fig. 7b that the percolation threshold of GC in the PHBV matrix is greater than that observed in the green LDPE matrix. According to Montanheiro et al. [42], the electrical resistivity of neat PHBV is around 2.0×10^{10} Ω m; that is, the electrical resistivity of the material is located in the upper boundary of the electrical resistivity range of antistatic materials (10^3–10^{10} Ω m) [17]. The addition of 1.0 wt% of GC to the PHBV matrix did not lead to any significant decrease in the electrical resistivity of PHBV. However, the addition of 2.5 wt% and 5.0 wt% GC content was responsible for the formation of an electron conduction path in the material, reducing the electrical resistivity of PHBV to 3.0×10^7 and 1.4×10^7 Ω m, respectively. The formation of electrical conduction path in PHBV composites is shown in the zoom of Fig. 7b. In this way, it is verified that the composites of green LDPE/GC with 0.1, 0.3, and 0.5 wt% GC and the composites of PHBV/GC with 2.5 and 5.0 wt% GC are materials that satisfy the electrical requirements to be classified as antistatic materials and may be used in the production of antistatic packaging. It is also verified that the 2.5 wt% GC content is the electrical percolation threshold of GC in PHBV matrix, which is slightly higher than the electrical percolation threshold of GC in green LDPE (0.1 wt%); that is, it is necessary to use smaller amounts of GC in green LDPE matrix to obtain materials with antistatic properties.

Santos et al. [54] produced composites of conventional LDPE with different GC contents (0.5, 1, 5, 10, 15, and 20 wt%) and also observed a relatively low electrical percolation threshold for GC (0.5 wt% GC) in the polymeric matrix, corroborating with the interesting results verified for the green LDPE/GC composites.

The biodegradation test in aqueous medium was performed only for neat PHBV and PHBV/2.5 GC composite, since it contained the lowest GC content necessary to impart antistatic properties to PHBV. Although green LDPE/GC composites present greater flexibility and a lower electrical percolation threshold than PHBV/GC composites, green LDPE/GC composites are recyclable, but not biodegradable materials. The PHBV/2.5 GC composites, on the other hand, present a good biodegradability, as shown in Fig. 8. Control samples (Fig. 8a, c) present homogeneous surface coloration and full physical integrity, while samples exposed to biodegradation in aqueous medium (Fig. 8b, d) present a lack of brightness and a loss in its surface homogeneity with the presence of cavities caused by the deterioration of the polymer matrix promoted by the action of the microorganisms.

Figure 9 shows the graph of the residual weight of neat PHBV and PHBV/2.5 GC composite as a function of biodegradation time. The samples of neat PHBV and PHBV/2.5 GC submitted to the biodegradation process in aqueous medium have a gradually decreasing weight over time. It is also observed that both neat PHBV and PHBV/2.5 GC composite show approximately the same decrease in weight (~52%) after 45 days of biodegradation in liquid medium, suggesting that the hydrophobic character of GC particles may not interfere in the microorganism's adhesion and proliferation on the PHBV matrix [7]. It is possible to suggest that in this biodegradation process, the microorganisms converted high molar mass polymer chains into

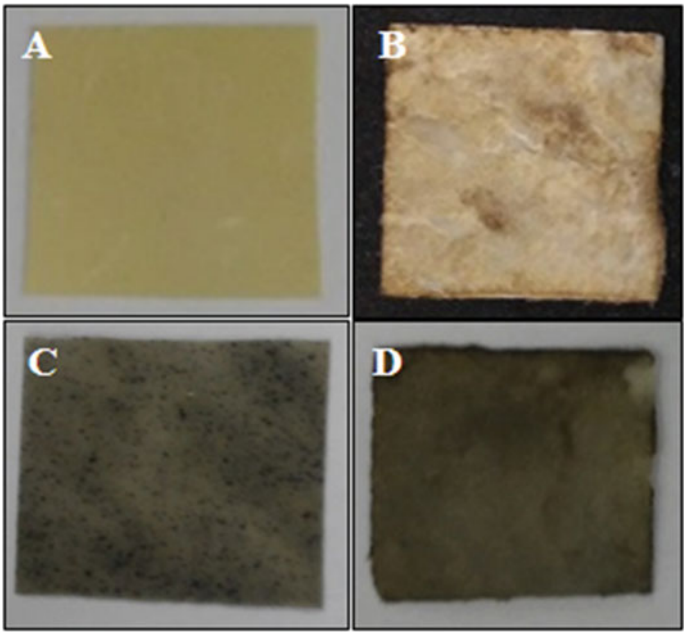

Fig. 8 Visual macroscopic analysis for neat PHBV: control neat PHBV sample (**a**) and neat PHBV exposed to biodegradation in aqueous medium during 45 days; control PHBV/2.5 GC (**c**) and PHBV/2.5 GC (**d**) exposed to biodegradation in aqueous medium during 45 days. *Source* Author

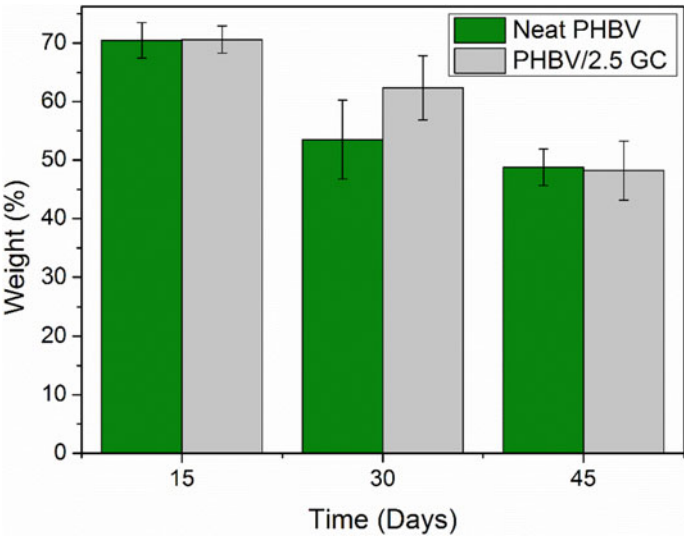

Fig. 9 Graph of residual weight of neat PHBV and PHBV/2.5 GC composite as a function of biodegradation time. *Source* Author

products of lower molar mass, such as water molecules and carbon dioxide, justifying the observed loss of weight [49].

4 Conclusions

The use of green composites is an interesting alternative for the production of antistatic packaging. These packaging must have low electrical resistivity to dissipate electrical charges through their structure and avoid damages in the electronic component.

Many techniques are studied to produce antistatic packaging like the addition of organic antistatic agents, such as ionic and non-ionic surfactants, metallic particles, metal oxide whiskers, the addition of intrinsically conducting polymers, use of conductive ionomers, the formation of polymeric electrolytes, and the addition of carbon materials like carbon black, carbon nanotubes, and glassy carbon (GC) in polymeric matrices. Among all these techniques, the use of an antistatic agent is an alternative that can be sustainable. GC can be used as an antistatic agent and is characterized as a carbon material originated from a renewable resource since it is obtained from the biomass of plants.

A sustainable way to produce antistatic packaging is using biodegradable or green polymers from renewable resources. Green LDPE and PHBV are promising alternatives to produce antistatic packaging with GC. The use of different polymeric matrices is an important step toward the diversification of the plastic market.

Mechanical, thermal, and electrical results confirm the good properties of these composites, and the low electrical resistivity can be reached with low contents of GC in green LDPE matrix (0.1–0.5 wt%) and PHBV matrix (2.5–5.0 wt%), especially when compared to carbon black (10–15 wt%). A reduction in electrical resistivity, on average of 99%, was achieved in both cases.

The use of biodegradable and green polymeric matrices is an advantage for the sector, contributing to the environment through the production of eco-friendly packaging.

Acknowledgements The authors are rather grateful to FAPESP (process 2018/09531-2), CNPq (Conselho Nacional de Desenvolvimento Científico e Tecnológico, process 310196/2018-3, 305123/2018-1), and the Coordenação de Aperfeiçoamento de Pessoal de Nível Superior—Brasil (CAPES)—Finance Code 001. The authors also thank Braskem (Brazil) for the donation of the Green LDPE.

References

1. Akaraonye E, Keshavarz T, Roy I (2010) Production of polyhydroxyalkanoates: the future green materials of choice. J Chem Technol Biotechn 85:732–743. https://doi.org/10.1002/jctb.

2392
2. Ambrosio-Martín J, Gorrasi G, Lopez-Rubio A et al (2015) On the use of ball milling to develop poly(3-hydroxybutyrate-co-3-hydroxyvalerate)-graphene nanocomposites (II)-Mechanical, barrier, and electrical properties. Appl Polym Sci 132: 42217. https://doi.org/10.1002/app.42217
3. ASTM (2014) D638-14: Standard Test Method for Tensile Properties of Plastics
4. ASTM (2018) D882-18: Standard Test Method for Tensile Properties of Thin Plastic Sheeting
5. Bao L, Lei J, Wang J (2013) Preparation and characterization of a novel antistatic poly(vinyl chloride)/quaternary ammonium based ion-conductive acrylate copolymer composites. J Electrostat 71:987–993. https://doi.org/10.1016/j.elstat.2013.09.001
6. Bélard L, Poncin-Epaillard F, Dole P et al (2013) Plasma-polymer coatings onto different biodegradable polyesters surfaces. Eur Polym 49:882–892. https://doi.org/10.1016/j.eurpolymj.2012.11.022
7. Belu AM, Guerrouani N, Baldo A et al (2007) Fluorinated-plasma coating on polyhydroxyalcanoate PHBV: effect on the biodegradation. J Fluor Chem 128:925–930. https://doi.org/10.1016/j.jfluchem.2007.03.018
8. Botelho EC, Scherbakoff N, Rezende MC (2001) Porosity control in glassy carbon by rheological study of the furfuryl resin. Carbon 39:45–52. https://doi.org/10.1016/S0008-6223(00)00080-4
9. Braga NF, LaChance AM, Liu B et al (2019) Influence of compatibilizer and carbon nanotubes on mechanical, electrical, and barrier properties of PTT/ABS blends. Adv Ind Eng Polym Res 2:121–125. https://doi.org/10.1016/j.aiepr.2019.07.002
10. Braskem (2020) Low density polyethylene SBF0323HC. https://www.braskem.com.br/busca-de-produtos?p=232. Accessed 10 Apr 2020
11. Callstrom MR, Neenan TX, McCreery RL et al (1990) Doped glassy carbon materials (DGC): low-temperature synthesis, structure, and catalytic behavior. J Am Chem Soc 112:4954–4956
12. Chan CM, Vandi LJ, Pratt S et al (2018) Mechanical properties of poly(3-hydroxybutyrate-co-3-hydroxyvalerate)/wood flour composites: effect of interface modifiers. J Appl Polym Sci 135:46828. https://doi.org/10.1002/app.46828
13. Chandra R, Rustgi R (1998) Biodegradable polymers. Prog Polym Sci 23:1273–1335
14. Che R, Yang W, Wang J et al (2010) Electrolyte-based antistatic plasticizer for soft poly(vinyl chloride) composites. J Appl Polym Sci 116:1718–1724. https://doi.org/10.1002/app.31600
15. Coutinho PLA, Morita AT, Cassinelli LF et al (2013) Braskem's ethanol to polyethylene process development. In: Imhof P, Waal JC (eds) Catalytic process development for renewable materials, 1st edn. Wiley-VCH, Weinheim, pp 149–166
16. Ding Y, Tang H, Zhang X et al (2008) Antistatic ability of 1-n-tetradecyl-3-methylimidazolium bromide and its effects on the structure and properties of polypropylene. Eur Polym J 44:1247–1251. https://doi.org/10.1016/j.eurpolymj.2008.01.030
17. ESD Association (2018) Part 3: basic ESD control procedures and materials. https://www.esda.org/esd-overview/esd-fundamentals/part-3-basic-esd-control-procedures-and-materials/. Accessed 10 Apr 2020
18. ESD Association (2020) Part 6: ESD Standards. https://www.esda.org/esd-overview/esd-fundamentals/part-6-esd-standards/. Accessed 10 Apr 2020
19. Feng X, Wang J, Zhang C (2018) Fabrication and characterization of antistatic epoxy composite with multi-walled carbon nanotube-functionalized melamine foam. RSC Adv 8:14740–14746. https://doi.org/10.1039/c8ra01044g
20. Ferrari PE, Rezende MC (1998) Carbono polimérico: processamento e aplicação. Polímeros 8:22–30. https://doi.org/10.1590/S0104-14281998000400005
21. Gaefke CB, Botelho EC, Ferreira NG et al (2007) Effect of furfuryl alcohol addition on the cure of furfuryl alcohol resin used in the glassy carbon manufacture. J Appl Polym Sci 106:2274–2281. https://doi.org/10.1002/app.26938
22. Ge C, Devar G (2017) Formation of polyvinyl alcohol film with graphene nanoplatelets and carbon black for electrostatic discharge protective packaging. J Electrostat 89:52–57. https://doi.org/10.1016/j.elstat.2017.07.004

23. Geyer R, Jambeck JR, Law KL (2017) Production, use, and fate of all plastics ever made. Sci Adv 3:25–29. https://doi.org/10.1126/sciadv.1700782
24. Gojny FH, Kopke U, Wichmanna MHG et al (2004) Carbon nanotube-reinforced epoxy-composites: enhanced stiffness and fracture toughness at low nanotube content. Compos Sci Technol 64:2363–2371. https://doi.org/10.1016/j.compscitech.2004.04.002
25. Harikrishnan G, Patro TU, Khakhar DV (2007) Reticulated vitreous carbon from polyurethane foam-clay composites. Carbon 45:531–535. https://doi.org/10.1016/j.carbon.2006.10.019
26. Huang HD, Liu CY, Zhang LQ et al (2015) Simultaneous reinforcement and toughening of carbon nanotube/cellulose conductive nanocomposite films by interfacial hydrogen bonding. ACS Sustain Chem Eng 3:317–324. https://doi.org/10.1021/sc500681v
27. Huang Y, Liu H, He P et al (2010) Nonisothermal crystallization kinetics of modified bamboo fiber/PCL composites. J Appl Polym Sci 116:2119–2125. https://doi.org/10.1002/app
28. Inagaki M, Kang F (2014) Materials science and engineering of carbon: fundamentals. Butterworth-Heinemann, Oxford
29. Jacobsen AJ, Mahoney S, Carter WB et al (2010) Vitreous carbon micro-lattice structures x. Carbon 49:1025–1032. https://doi.org/10.1016/j.carbon.2010.10.059
30. Jenkins GM, Kawamura K (1971) Structure of glassy carbon. Nature 231:175–176. https://doi.org/10.1038/231175a0
31. Jenkins GM, Kawamura K (1976) Polymeric carbons: carbon fibre, glass and char. Cambridge University Press, Cambridge
32. Jiang N, Abe H (2015) Crystallization and mechanical behavior of covalent functionalized carbon nanotube/poly (3-hydroxybutyrate-co-3-hydroxyvalerate) nanocomposites. J Appl Polym Sci 132:42136. https://doi.org/10.1002/app.42136
33. Jonas F, Heywang G (1994) Technical applications for conductive polymers. Electrochim Acta 39:1345–1347
34. Kalijadis A, Jovanović Z, Laušević M et al (2011) The effect of boron incorporation on the structure and properties of glassy carbon. Carbon 49:2671–2678. https://doi.org/10.1016/j.carbon.2011.02.054
35. Lemes AP, Soto-Oviedo MA, Waldman WR et al (2010) Effect of lignosulfonate on the thermal and morphological behavior of poly(3-hydroxybutyrate-co-3-hydroxyvalerate). J Polym Environ 18:250–259. https://doi.org/10.1007/s10924-010-0170-7
36. Lemes AP, Montanheiro TLA, Passador FR et al (2014) Nanocomposites of polyhydroxyalkanoates reinforced with carbon nanotubes: chemical and biological properties. In: Thakur VK, Thakur MK (eds) Eco-friendly polymer nanocomposites: processing and properties. Springer, New Delhi, pp 79–108
37. Lucas N, Bienaime C, Belloy C et al (2008) Polymer biodegradation: mechanisms and estimation techniques. Chemosphere 73:429–442. https://doi.org/10.1016/j.chemosphere.2008.06.064
38. Luckachan GE, Pillai CKS (2011) Biodegradable polymers—a review on recent trends and emerging perspectives. J Polym Environ 19:637–676. https://doi.org/10.1007/s10924-011-0317-1
39. Maki N, Nokano S, Sasaki H (2004) Development of a packaging material using non-bleed-type antistatic ionomer. Packag Technol Sci 17:249–256. https://doi.org/10.1002/pts.653
40. Modi S, Koelling K, Vodovotz Y (2011) Assessment of PHB with varying hydroxyvalerate content for potential packaging applications. Eur Polym J 47:179–186. https://doi.org/10.1016/j.eurpolymj.2010.11.010
41. Montané D, Salvadó J, Torras C et al (2002) High-temperature dilute-acid hydrolysis of olive stones for furfural production. Biomass Bioenerg 22:295–304. https://doi.org/10.1016/S0961-9534(02)00007-7
42. Montanheiro TLA, Cristóvan FH, Machado JPB et al (2014) Effect of MWCNT functionalization on thermal and electrical properties of PHBV/MWCNT nanocomposites. J Mater Res 30:55–65. https://doi.org/10.1557/jmr.2014.303
43. Morschbacker A, Campos CES, Cassiano LC et al (2014) Bio-polyethylene. In: Oksman K, Mathew AP, Bismarck A et al (eds) Handbook of green materials, vol 4. World Scientific Publishing Company, California, pp 89–104

44. Nel A, Xia T, Mädler L et al (2006) Toxic potential of materials at the nanolevel. Science 311:622–627. https://doi.org/10.1126/science.1114397
45. Oishi SS, Botelho EC, Rezende MC et al (2017) Structural and surface functionality changes in reticulated vitreous carbon produced from poly(furfuryl alcohol) with sodium hydroxide additions. Appl Surf Sci 394:87–97. https://doi.org/10.1016/j.apsusc.2016.10.112
46. Oyama IC, de Souza GPM, Rezende MC et al (2020) A new eco-friendly green composite for antistatic packaging: green low-density polyethylene/glassy carbon. Polym Compos. https://doi.org/10.1002/pc.25572
47. Pandit JA, Sudarshan K, Athawale AA (2016) Electrically conductive epoxy-polyester-graphite nanocomposites modified with aromatic amines. Polymer 104:49–60. https://doi.org/10.1016/j.polymer.2016.09.084
48. Raza ZA, Abid S, Banat IM (2018) Polyhydroxyalkanoates: characteristics, production, recent developments and applications. Int Biodeterior Biodegrad 126:45–56. https://doi.org/10.1016/j.ibiod.2017.10.001
49. Rizzarelli P, Carroccio S (2014) Modern mass spectrometry in the characterization and degradation of biodegradable polymers. Anal Chim Acta 808:18–43. https://doi.org/10.1016/j.aca.2013.11.001
50. Rupp B, Ebner C, Rossegger E et al (2010) UV-induced crosslinking of the biopolyester poly(3-hydroxybutyrate)-co-(3-hydroxyvalerate). Green Chem 12:1796–1802. https://doi.org/10.1039/c0gc00066c
51. Sakintuna B, Yürüm Y (2005) Templated porous carbons: a review article. Ind Eng Chem Res 44:2893–2902. https://doi.org/10.1021/ie049080w
52. Salomez M, George M, Fabre P et al (2019) A comparative study of degradation mechanisms of PHBV and PBSA under laboratory-scale composting conditions. Polym Degrad Stab 167:102–113. https://doi.org/10.1016/j.polymdegradstab.2019.06.025
53. Sandler JKW, Kirk JE, Kinloch IA et al (2003) Ultra-low electrical percolation threshold in carbon-nanotube-epoxy composites. Polymer 44:5893–5899. https://doi.org/10.1016/S0032-3861(03)00539-1
54. Santos MS, Montagna LS, Rezende MC et al (2018) A new use for glassy carbon: development of LDPE/glassy carbon composites for antistatic packaging applications. J Appl Polym Sci 136:47204. https://doi.org/10.1002/app.47204
55. Shah AA, Hasan F, Hameed A et al (2008) Biological degradation of plastics: a comprehensive review. Biotechnol Adv 26:246265. https://doi.org/10.1016/j.biotechadv.2007.12.005
56. Sharma S (2018) Glassy Carbon: a promising material for micro and nanomanufacturing. Materials 11:1857. https://doi.org/10.3390/ma11101857
57. Silva LN, dos Anjos EGR, Morgado GFM et al (2019) Development of antistatic packaging of polyamide 6/linear low-density polyethylene blends-based carbon black composites. Polym Bull. https://doi.org/10.1007/s00289-019-02928-3
58. Silva TF, Menezes F, Montagna LS et al (2018) Preparation and characterization of antistatic packaging for electronic components based on poly(lactic acid)/carbon black composites. J Appl Polym Sci 136:47273. https://doi.org/10.1002/app.47273
59. Silva AP, Montanheiro TLA, Montagna LS et al (2019) Effect of carbon nanotubes on the biodegradability of poly (3-hydroxybutyrate-co-3-hydroxyvalerate) nanocomposites. J Appl Polym Sci 136:48020. https://doi.org/10.1002/app.48020
60. Sun Q, Li W (2016) Inorganic-Whisker-reinforced polymer composites: synthesis, properties and applications. CRC Press, London
61. SPI Supplies (2020) Glassy carbon. https://www.2spi.com/category/labware-crucibles-glassy-carbon/labware/. Accessed 15 Apr 2020
62. Szeluga U, Kumanek B, Trzebicka B (2015) Synergy in hybrid polymer/nanocarbon composites. A review. Compos Part A 73:204–231. https://doi.org/10.1016/j.compositesa.2015.02.021
63. Szeluga U, Pusz S, Kumanek B et al (2016) Influence of unique structure of glassy carbon on morphology and properties of its epoxy-based binary composites and hybrid composites with carbon nanotubes. Compos Sci Technol 134:72–80. https://doi.org/10.1016/j.compscitech.2016.08.004

64. Tian Y, Zhang X, Geng HZ et al (2017) Carbon nanotube/polyurethane films with high transparency, low sheet resistance and strong adhesion for antistatic application. RSC Adv 7:53018–53024. https://doi.org/10.1039/c7ra10092b
65. Turan D, Sirin H, Ozkoc G (2011) Effects of POSS particles on the mechanical, thermal, and morphological properties of PLA and plasticised PLA. J Appl Polym Sci 121:1067–1075. https://doi.org/10.1002/app
66. Vidhate S, Innocentini-Mei L, D'Souza NA (2012) Mechanical and electrical multifunctional poly(3-hydroxybutyrate-co-3-hydroxyvalerate)-multiwall carbon nanotube nanocomposites. Polym Eng Sci 56:1367–1374. https://doi.org/10.1002/pen.23084
67. Wang Y, Zhang C, Du Z et al (2013) Synthesis of silver nanoparticles decorated MWCNTs and their application in antistatic polyetherimide matrix nanocomposite. Synth Met 182:49–55. https://doi.org/10.1016/j.synthmet.2013.09.006
68. Wang H, Xie G, Fang M et al (2015) Electrical and mechanical properties of antistatic PVC films containing multi-layer graphene. Compos Part B Eng 79:444–450. https://doi.org/10.1016/j.compositesb.2015.05.011
69. Wang J, Bao L, Zhao H et al (2012) Preparation and characterization of permanently anti-static packaging composites composed of high impact polystyrene and ion-conductive polyamide elastomer. Compos Sci Technol 72:976–981. https://doi.org/10.1016/j.compscitech.2012.03.006
70. Wang J, Che R, Yang W et al (2011) Biodegradable antistatic plasticizer based on citrate electrolyte doped with alkali metal salt and its poly(vinyl chloride) composites. Polym Int 60:344–352. https://doi.org/10.1002/pi.2952
71. Weng YX, Wang Y, Wang XL et al (2010) Biodegradation behavior of PHBV films in a pilot-scale composting condition. Polym Test 29:579–587. https://doi.org/10.1016/j.polymertesting.2010.04.002
72. Wypych G (2012) Handbook of polymers. ChemTec Publishing, Toronto
73. Zhang X, Liu J, Wang Y et al (2017) Effect of polyamide 6 on the morphology and electrical conductivity of carbon black-filled polypropylene composites. R Soc Open Sci 4:170769. https://doi.org/10.1098/rsos.170769
74. Zheng W, Chen WG, Ren SX et al (2019) Interfacial structures and mechanisms for strengthening and enhanced conductivity of graphene/epoxy nanocomposites. Polymer 163:171–177. https://doi.org/10.1016/j.polymer.2018.12.055
75. Zhou Z, Chu L, Tang W et al (2003) Studies on the antistatic mechanism of tetrapod-shaped zinc oxide whisker. J Electrostat 57:347–354. https://doi.org/10.1016/S0304-3886(02)00171-7
76. Zhu Y, Zhao Y, Zhang X et al (2016) Metal filaments/nano-filler filled hybrid polymer fibers with improved conductive performance. Mater Lett 173:26–30. https://doi.org/10.1016/j.matlet.2016.03.007